Large two-photon absorptivity of hemoglobin in the infrared range of 780–880 nm

G. Omar Clay, Chris B. Schaffer,[a] and David Kleinfeld[b]
Department of Physics, University of California at San Diego, La Jolla, California 92093

(Received 1 September 2006; accepted 10 November 2006; published online 11 January 2007)

Porphyrin molecules have a highly conjugated cyclic structure and are theorized to have unusually large two-photon absorptivities (σ_{TPA}), i.e., $\sigma_{TPA} \sim 10^2$ GM. The authors tested this claim. Ultrafast two-photon absorption (TPA) spectroscopy was performed on solutions of hemoglobin, which contains a naturally occurring metaloporphyrin. They used a pump-probe technique to directly detect the change in transmission induced by TPA over the wavelength range of $\lambda_0 = 780-880$ nm. As controls, they measured the TPA of the dyes rhodamine 6G and B; their measurements both verify and extend previously reported values. In new results, hemoglobin was found to have a peak two-photon absorptivity of $\sigma_{TPA} \sim 150$ GM at $\lambda_0 = 825$ nm, near a resonance of the Soret band. This value supports theoretical expectations. They also found a significant difference in the TPA of carboxyhemoglobin versus oxyhemoglobin, e.g., $\sigma_{TPA} = 61$ GM versus $\sigma_{TPA} = 18$ GM, respectively, at $\lambda_0 = 850$ nm, which shows that the ligand affects the electronic states involved in TPA. © *2007 American Institute of Physics*. [DOI: 10.1063/1.2404678]

Two-photon absorption (TPA) provides a means to measure electronic transitions that cannot be studied with one-photon processes and, with advent of nonlinear laser scanning microscopy, provides a basis for contrast in biological imaging. Presently, the primary approach to investigate solution-phase TPA that is driven by ultrafast, i.e., ~100 fs, duration laser pulses, is via two-photon excited fluorescence (TPEF). However, the interpretation of these measurements requires assumptions with regard to the yield of TPEF versus nonradiative decay and is clearly limited to use with fluorescent materials.

Two-photon absorption in nonfluorescent biomolecules is of interest theoretically and of practical importance. In particular, molecular orbital calculations on porphyrins predict that a number of Soret band states have two-photon absorptivities that exceed $100\ \text{GM} = 10^{-48}\ \text{cm}^4\ \text{s/(molecule photon)}$.[1] This value is achieved in synthetic systems for asymmetrically substituted monomeric porphyrins[2] as well as in *n*-mers of porphyrins linked via saturated bonds.[3,4] Two-photon absorption by the metaloporphyrin-containing protein hemoglobin is of special interest from the perspective of physiology. First, *in vivo* studies of cortical blood flow depend on TPEF laser scanning microscopy as a means to image flow of unlabeled blood cells that move against fluorescently labeled blood plasma.[5–11] Second, TPA by hemoglobin is considered both a possible route for photodamage and a potential contrast mechanism to report blood oxygenation.

Here, we performed nonlinear transmission measurements on hemoglobin in solution at the physiologically relevant concentration of 2 mM, i.e., ~17 g/dl, which corresponds to the *average* concentration in blood; the concentration in red blood cells is about two times higher. We measured TPA in a 98% (v/v) oxyhemoglobin (HbO_2) solution and a mixed 60% (v/v) carboxyhemoglobin/oxyhemoglobin (HbCO) solution (Nos. 300881R0 and 300879R0, respectively; Instrumentation Laboratories). In order to compare our TPA measurement technique with the few existing studies that have directly characterized TPA rather than TPEF,[12–14] we also investigated TPA in 8.3 mM solutions of rhodamine 6G (No. R4127-100G; Sigma-Aldrich) and rhodamine B chloride (No. R-6626; Sigma-Aldrich) in methanol. In all cases, our sample containers were microcuvettes (No. 3520; Vitrocom) with flat, 200 μm thick glass (Duran type 8340) walls and a 200 μm wide internal chamber.

We used the double modulation variant of pump-probe spectroscopy described by Frolov and Vardeny[15] as a means to directly detect TPA in solution-phase material. Our laser source was a variable wavelength Ti:sapphire oscillator (Mira 900-F with 10 W Verdi pump; Coherent Inc.) with a 76 MHz repetition rate. The laser beam was divided into a pump and a probe beam. An acoustic optical modulator (AOM) (No. 1205C-2; Isomet) was used to impose a 0.62 MHz modulation to the pump beam, a dual beam mechanical chopper (No. 3501; New Focus) imparted an additional 3.2 kHz modulation to the pump and a 4.5 kHz modulation to the probe beam. Autocorrelation of both beams revealed a temporally Gaussian pulse profile. The duration of the probe pulse was ~100 fs while that of the pump was stretched by dispersion in the AOM to ~200 fs. The beams were cofocused (0.3 NA 10× Neofluar; Zeiss) in the sample and collected independently with a pair of reverse biased photodiodes (Det210; Thorlabs). We then downconverted the probe signal electronically (No. ZP3 Mixer; MiniCircuits) at

[a]Present address: Department of Biomedical Engineering, Cornell University, 120 Olin Hall, Ithaca, NY 14853.
[b]Author to whom correspondence should be addressed. Tel.: 858-822-0342. Fax: 858-534-7697. Electronic mail: dk@physics.ucsd.edu

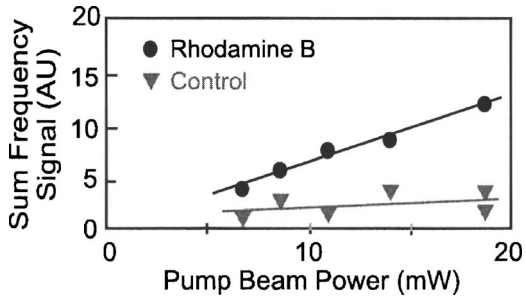

FIG. 1. A single-trial TPA measurement on rhodamine B (8.3 mM in methanol) at $\lambda_0=880$ nm shows the linearity of the sum-frequency signal with the pump beam power. Control data are collected with the rhodamine sample placed in the beam path but outside of the focal region.

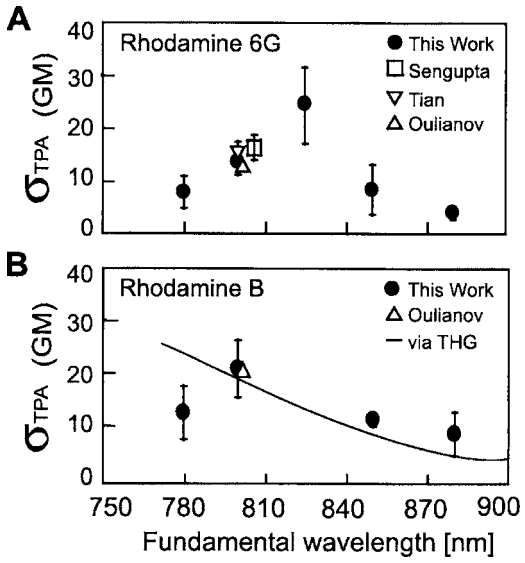

FIG. 2. The two-photon absorptivity [Eq. (4)] of 8.3 mM solutions of rhodamine 6G [panel (A)] and rhodamine B [panel (B)] in methanol is shown along with previously measured values by Sengupta *et al.* (10 mM) (Ref. 12), Tian and Warren (30 mM) (Ref. 13), and Oulianov *et al.* (20 and 23 mM, respectively) (Ref. 14) In panel (B), the curve represents two-photon enhanced THG from a 1 mM aqueous solution of rhodamine B (Ref. 19). The THG curve has been amplitude scaled.

0.62 MHz and used phase-sensitive detection (No. SR530; Stanford Research Systems) to phase lock to the audio frequency sum-frequency signal at 7.6 kHz. This process sensitively detected changes in the intensity of the transmitted probe beam that were caused by optical mixing of the probe beam with the pump beam. The double modulation approach enhanced the signal-to-noise ratio by modulating the beam at 0.62 MHz, where laser noise is minimal, and then electronically mixing back down to 7.6 kHz, where the superior signal-to-noise ratio of audio frequency lock-in amplifiers can be retained.

The sum-frequency signal represents multiphoton events in which at least one photon is recruited from each of the pump and the probe pulses. The sum-frequency signal is proportional to TPA events provided that, first, we collect all of the transmitted probe light to avoid systematic complications that stem from the nonlinear index and, second, that the excitation power is limited such that excited state absorption and higher-order nonlinearities are not significantly recruited. Under these conditions, the sum-frequency signal increases linearly with the optical power in the pump beam (Fig. 1). The fractional uncertainty in the slope of this linear relation, as an average over trials, comprised the dominant source of error in our determination of the absorptivity (Figs. 2 and 3).

Samples were mounted on a stage and could be translated along the optical axis of the objective (z scanned). Two-photon excited fluorescence while z scanning was used to estimate the axial extent of the overlap volume of the cofocused beams in a fluorescent sample. We found an effective axial overlap, denoted L, of $L=94$ μm at the $1/e$ point. Typical TPA measurements were performed by positioning the sample at the center of the focus and recording the difference in the sum-frequency signal when the beams were temporally overlapped, and when the pump pulse lagged the probe in time by about ~5 ps. Differencing in this way controlled for background offset in the detection scheme. The measurement was performed at various pump powers and the resulting differential sum-frequency signal versus pump power data fitted with a line.

A thin plate of gallium phosphide (GaP) was used for absolute calibration of the transmission change measured with the pump-probe technique. The fractional intensity loss of the transmitted probe beam induced by mixing with the pump beam, denoted $\Delta T/T$, can be directly measured in GaP.[16,17] We use phase-sensitive detection and lock to the modulation frequency of the beam probe. The difference, ΔT, corresponds to the detection output for temporally separated probe and pump pulses minus the case of coincident pulses. Typical values of $(\Delta T/T)_{\mathrm{GaP}}$ for GaP were found to range between 1.5×10^{-3} and 8×10^{-3} for a pump power at the focus of the beam, denoted P_{ref}, in the range $P_{\mathrm{ref}}=20-50$ mW, with an uncertainty of less than 6%. This allowed us to equate the power dependent slope of the differenced sum-frequency signal from GaP, denoted V_{GaP}, to the absolute change in transmission of the probe beam, $(\Delta T/T)_{\mathrm{GaP}}$, thereby providing absolute calibration for our sum-frequency measurements. The fractional intensity loss of each sample at pump power P_{ref}, denoted $(\Delta T/T)_{\mathrm{sample}}$, was then determined by taking the ratio of the measured power dependent slope of the sum-frequency signal from the sample, denoted V_{sample}, to that of GaP, denoted V_{GaP}, and then multiplying by $(\Delta T/T)_{\mathrm{GaP}}$, i.e.,

$$\left(\frac{\Delta T}{T}\right)_{\mathrm{sample}}=\frac{V_{\mathrm{sample}}}{V_{\mathrm{GaP}}}\left(\frac{\Delta T}{T}\right)_{\mathrm{GaP}}. \tag{1}$$

In this manner we routinely measured fractional sensitivities of $(\Delta T/T)_{\mathrm{sample}}\sim5\times10^{-6}$ for molecules in solution, which compares favorably with the sensitivity previously achieved with this scheme for thin films.[15] The uncertainty in $(\Delta T/T)_{\mathrm{sample}}$ was dominated by the trial-to-trial variability in measurements of V_{sample} and ranged from 6% to 53%, with a mean value of 23%.

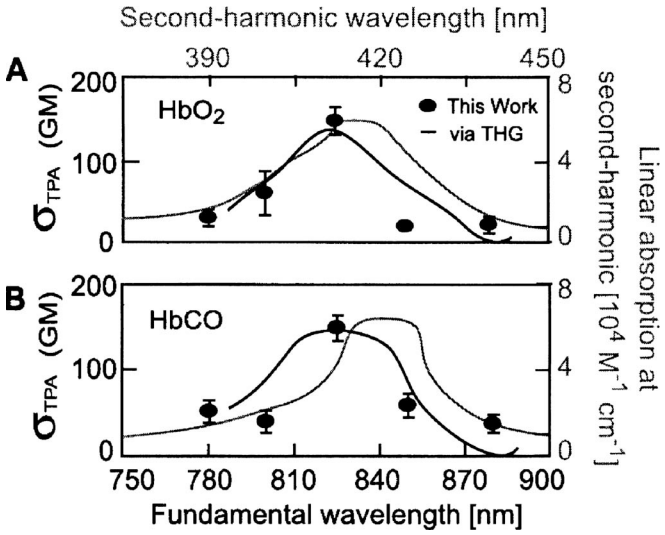

FIG. 3. The two-photon absorptivity [Eq. (4)] of HbO_2 [panel (A)] and HbCO [panel (B)] is plotted (left-hand scale) along with the linear absorption coefficient (gray lines, right-hand scale) at twice the incident photon energy (upper wavelength scale). A statistically significant difference in the TPA of HbO_2 and HbCO is found at $\lambda_0=850$ nm. Systematic uncertainties are not included in the error bars. The dark lines represent amplitude scaled, TPA resonance enhanced THG spectra of the same solutions (Ref. 19). The THG curves have been amplitude scaled.

Optical absorption proceeds according to the relation

$$\frac{dI}{dz} = \alpha I + \beta I^2, \tag{2}$$

where I is the incident intensity, z is the optical path length, α is the one-photon absorption coefficient, and β is the two-photon absorption coefficient. The two-photon absorptivity, denoted σ_{TPA}, is proportional to the two-photon absorption coefficient, i.e.,

$$\sigma_{TPA} = \frac{\hbar\omega}{N}\beta, \tag{3}$$

where $\hbar\omega$ is the energy of the excitation photon and N is the number density of scatters. The two-photon absorptivity is further related to the fractional change in transmission $\Delta T/T$ of the probe induced by the pump by[18]

$$\sigma_{TPA} = \frac{\hbar\omega}{N}\frac{1+\eta}{\sqrt{2}\eta}\frac{A}{L}\frac{1}{P_{ref}}\left(\frac{\Delta T}{T}\right)_{sample} = \frac{\hbar\omega}{N}\frac{1+\eta}{\sqrt{2}\eta}\frac{A}{L}\frac{1}{P_{ref}}\frac{V_{sample}}{V_{GaP}}\left(\frac{\Delta T}{T}\right)_{GaP}, \tag{4}$$

where $\eta \approx 0.69$ is the ratio of the cross-sectional areas of the pump to the probe beams and A is an effective cross-sectional area of the overlap volume of the beams at the focus. The area A is estimated in two ways. First, through the relation $A=\lambda_0 b/(2n)$, where λ_0 is the center wavelength of the pulse and b is the confocal parameter of a single beam; the parameter b is measured through z scanning while electronically locking onto the beam of interest. Second, the parameter A is estimated through the relation $A=(\lambda_0^2/\pi)(1-NA_{eff}^2)/NA_{eff}^2$ where $NA_{eff}=NA$ (beam size)/(back aperture size) and NA is the stated numerical aperture of the air objective. The relations for A were evaluated by measuring the ratio of the beam areas at the back aperture of the excitation objective with the area of the back aperture. These two methods each yield $A/L=5\pm1$ μm. The estimation of parameters for Eq. (4) introduces a total systematic error in the value of σ_{TPA} of approximately 18%. The error bars for the data in Figs. 2 and 3 only capture measurement error, with a mean of 23% as noted above, and do not reflect systematic errors.

Our measurements of TPA in rhodamines 6G and B at 800 nm, i.e., $\sigma_{TPA}=13.4$ GM and $\sigma_{TPA}=21$ GM, respectively, are in excellent correspondence with previous direct TPA measurements[12–14] at similar concentrations (Fig. 2). We also measure TPA in these dyes at other wavelengths between 780 and 880 nm (Fig. 2). Third harmonic generation (THG) microspectroscopy studies[19] on an aqueous solution of rhodamine B show a TPA resonance with a similar, though not exactly conforming, spectral profile to what we find here [black line in Fig. 2(b)]. Naive comparisons with existing TPEF measurements made with solutions of rhodamine, typically at concentrations of 100 μM or less, are inappropriate in light of the complex concentration dependence of TPEF in these dyes.[20]

For hemoglobin, the TPA spectra roughly track the linear absorption at half the wavelength (Fig. 3), as might be expected for two-photon absorption dominated by a two-photon resonance. Hemoglobin has a peak in TPA at $\lambda_0=825$ nm, with $\sigma_{TPA}=150$ GM. The two-photon peak corresponds to a one-photon absorption peak at 420 nm [Figs. 3(a) and 3(b)], which is assigned to the Soret band. The approximately 15 nm blueshift in the measured TPA peak compared to the location expected from the position of the linear absorption peak at half the wavelength [gray curves in Figs. 3(a) and 3(b)] is also detected in TPA resonance enhanced THG spectra of the same solutions [black curves in Figs. 3(a) and 3(b)].[19] Similar shifts in TPA peaks have been observed in TPEF measurements of autofluorescent proteins.[21] Even off of resonance, the TPA of hemoglobin is substantial, e.g., $\sigma_{TPA}=20-60$ GM. The observation that both THG (Ref. 19) and TPA (Fig. 3) in hemoglobin have spectral profiles with a peak near 825 nm suggests that a TPA resonance enhancement due to the Soret band is an important mechanism in both of these processes. While nonresonant mechanisms may contribute, our interpretation is consistent with theoretical and related experimental findings.[1,22]

Our data conform theoretical expectations of large two-photon absorptivities in porphyrins as a result of Soret band states.[1] The TPA resonance appears less prominent than its one-photon counterpart, a feature also noticed in the third harmonic studies.[19] The two ligand states HbO_2 and HbCO have small but significantly different two-photon absorptivities near the edge of the resonance band that is centered at $\lambda=850$ nm. A similar difference, albeit at 875 nm rather than 850 nm, was inferred from THG spectra.[19] Thus the nonlinear optical properties of hemoglobin may be used to distinguish among oxidation states.

The large two-photon absorptivity and relatively high concentration of hemoglobin in red blood cells, ~4 mM,

support the contention that these cells may be good candidates for nonlinear imaging and spectroscopy studies *in vivo*. On resonance, i.e., $\lambda_0=825$ nm, and at the highest imaging powers, i.e., $I\sim 5\times 10^{11}$ W/cm^2, the energy deposition in a red blood cell at the focus that results from TPA in hemoglobin approaches that due to one-photon absorption, i.e., $\beta I/\alpha\sim 1$ [Eq. (2)]. This suggests that under focused high intensity illumination, TPA in hemoglobin may provide a basis for imaging contrast that rivals that of linear processes.

The authors acknowledge discussions and technological support from Peifang Tian, Philbert Tsai, and Earl Dolnick and editorial comments from Grover Swartzlander. They thank the David and Lucille Packard Foundation (99-8326), the National Institutes for Biomedical Imaging and Bioengineering (EB003832), and the National Center for Research Resources (RR021907) for support.

[1] M. B. Masthay, L. A. Findsen, B. M. Pierce, D. F. Bocian, J. S. Lindsey, and R. R. Birge, J. Chem. Phys. **84**, 3901 (1986).
[2] M. Drobizhev, F. Meng, A. Rebane, Y. Stepanenko, E. Nickel, and C. W. Spangler, J. Phys. Chem. B **110**, 9802 (2006).
[3] M. Drobizhev, Y. Stepanenko, Y. Dzenis, A. Karotki, A. Rebane, P. N. Taylor, and H. L. Anderson, J. Am. Chem. Soc. **126**, 15352 (2004).
[4] X. Zhou, A.-M. Ren, J.-K. Feng, X.-J. Liu, and Y.-D. Zhang, ChemPhysChem **4**, 991 (2003).
[5] D. Kleinfeld, P. P. Mitra, F. Helmchen, and W. Denk, Proc. Natl. Acad. Sci. U.S.A. **95**, 15741 (1998).
[6] E. Chaigneau, M. Oheim, E. Audinat, and S. Charpak, Proc. Natl. Acad. Sci. U.S.A. **100**, 13081 (2003).
[7] B. A. Flusberg, J. C. Jung, E. D. Cocker, E. P. Anderson, and M. J. Schnitzer, Opt. Lett. **30**, 2272 (2005).
[8] W. Gobel, J. N. Kerr, A. Nimmerjahn, and F. Helmchen, Opt. Lett. **29**, 2521 (2004).
[9] E. B. Hutchinson, B. Stefanovic, A. P. Koretsky, and A. C. Silva, Neuroimage **32**, 520 (2006).
[10] C. B. Schaffer, B. Friedman, N. Nishimura, L. F. Schroeder, P. S. Tsai, F. F. Ebner, P. D. Lyden, and D. Kleinfeld, PLoS Biol. **4**, 258 (2006).
[11] P. Theer, M. T. Hasan, and W. Denk, Opt. Lett. **28**, 1022 (2003).
[12] P. Sengupta, J. Balaji, S. Banerjee, R. Philip, R. Kumar, and S. Maiti, J. Chem. Phys. **112**, 9201 (2000).
[13] P. Tian and W. Warren, Opt. Lett. **27**, 1634 (2002).
[14] D. A. Oulianov, A. S. Tomov, A. S. Dvornikov, and P. M. Rentzepis, Opt. Commun. **191**, 235 (2001).
[15] S. Frolov and Z. Vardeny, Rev. Sci. Instrum. **69**, 1257 (1998).
[16] J. H. Yee and H. H. M. Chau, Opt. Commun. **10**, 56 (1974).
[17] I. M. Catalano, A. Cingolani, and A. Minafra, Solid State Commun. **16**, 417 (1965).
[18] R. L. Sutherland, *Handbook of Nonlinear Optics* (Dekker, New York, 2003).
[19] G. O. Clay, A. C. Millard, C. B. Schaffer, J. Aus-der-Au, P. S. Tsai, J. A. Squier, and D. Kleinfeld, J. Opt. Soc. Am. B **23**, 932 (2006).
[20] N. K. M. N. Srinivas, S. V. Rao, and D. N. Rao, J. Opt. Soc. Am. B **20**, 2470 (2003).
[21] G. A. Blab, P. H. M. Lommerse, L. Cognet, G. S. Harms, and T. Schmidt, Chem. Phys. Lett. **350**, 71 (2001).
[22] S. Shima, R. P. Ilagan, N. Gillespie, B. J. Sommer, R. G. Hiller, F. P. Sharples, H. A. Frank, and R. R. Birge, J. Phys. Chem. A **107**, 8052 (2003).